# TRACKING OF SHEAR BANDS IN AN ANTIPLANE SHEAR MODEL

F. XABIER GARAIZAR AND JOHN TRANGENSTEIN

## 1. Introduction

In this notice we describe a numerical algorithm for the solution of a granular flow problem in two dimensions where shear bands are present. The main difficulty in this problem is the resolution of the motion near the shear band. In this region, traditional methods break down and a new approach, incorporating ideas from front-tracking techniques, is used.

We consider elasto-plastic deformations in an antiplane shear motion. That is, while the deformation is homogeneous in the $z$-direction (the state variables only depend on $x$ and $y$) the motion is only in the $z$-direction. In other words, the only non-trivial component of the velocity vector is in the $z$-direction.

When the material reaches a critical value of loading, shear banding occurs. While the overall deformation is described by a hyperbolic system of equations, hyperbolicity is lost at the points when shear banding occurs. At these points, the deformation is described by jump relations in a manner similar to shock-hugoniots. From a numerical point of view, shear bands are treated as internal boundaries.

An added problem is that the endpoints of the band can propagate at a rate that can be larger than the elastic speed. Effectively this means that the growth of the band is not limited by the CFL condition and the endpoints of a band can propagate across several cells during a single time-step. We update the cells where the shear band is likely to grow, and those where it already exists, at fractional time-steps allowing for the proper growth of the band.

## 2. Equations

We study a problem that models antiplane shearing as described in [7]. This motion is described by three unknowns: the $z$-component of the velocity, which we write as a scalar velocity $v$, and the $T_{31}$ and $T_{32}$ components of the Cauchy stress tensor $T$. We define a dimensionless stress vector $\vec{\tau} = (\tau_1, \tau_2)^T$ by identifying $\tau_1 = T_{31}$ and $\tau_2 = T_{32}$.

The equations governing the motion are: the momentum equation

$$\partial_t v = c^2 \text{ div } \vec{\tau} \ , \tag{1}$$

where $c$ is the speed of elastic waves, and the constitutive relations. These relations take different form for elastic and plastic deformations :

$$\partial_t \vec{\tau} = \text{grad } v \quad \text{if elastic} \tag{2}$$

$$\left( I + \frac{1}{h(|\vec{\tau}|) + |\vec{\tau}|^2 \cos\alpha} R \right) \partial_t \vec{\tau} = \text{grad } v \quad \text{if plastic.} \tag{3}$$

First author supported by NSF Grant DMS 9201115, which includes funds from AFOSR

Second author supported by NSF Grants DMS 9201034, DMS 9201361,DMS 9407029, and DOE Grant DE-F605-92-ER25145

Here $R$ is the rotation matrix $\begin{pmatrix} \cos\alpha & \sin\alpha \\ -\sin\alpha & \cos\alpha \end{pmatrix}$ and $h(|\vec{\tau}|)$ is the hardening modulus, which we assume satisfies $h' < 0$ and $h(1) = 0$. The parameter $\alpha$ in the rotation matrix $R$ characterizes the degree of non-associativity in the model.

The change from elastic to plastic behavior is described in terms of a yield condition of Von-Misses type. We say that the material is deforming plastically if $\partial_t|\vec{\tau}(t,x,y)| > 0$ and $|\vec{\tau}(t,x,y)| = \max_{0\leq s\leq t}(|\vec{\tau}(s,x,y)|)$, otherwise we say that the material is deforming elastically. For later use we define a measure of the accumulated stress as $\gamma(t,x,y) = \max_{0\leq s\leq t}(|\vec{\tau}(s,x,y)|)$.

For most of what follows it will be more convenient to write system (1)-(3) in quasilinear form:

$$\partial_t v = c^2 \operatorname{div}\vec{\tau} \tag{4}$$

$$\partial_t \vec{\tau} = A(\vec{\tau})\operatorname{grad} v \tag{5}$$

where $A(\vec{\tau}) = I$ if the deformation is elastic and $A(\vec{\tau}) = I - (h + |\vec{\tau}|^2\cos(\alpha))^{-1}R\vec{\tau}\vec{\tau}^T$ if the deformation is plastic. As noted in [7] the formation of shear bands is related to the ill-posedness of the problem, which occurs when speeds of planar waves, in some direction, become complex. For a given direction $\vec{\xi}$, the equations for planar waves propagating in that direction (i.e.; $(x,y) = s\vec{\xi}$), simplify to:

$$\partial_t v = c^2\,\partial_s(\vec{\xi}\cdot\vec{\tau}) \tag{6}$$

$$\partial_t\vec{\tau} = \vec{b}\,\partial_s v \tag{7}$$

where $\vec{b}$ is defined as $\vec{b}(\vec{\xi}) = \vec{\xi} - (h + |\vec{\tau}|^2\cos(\alpha))^{-1}R\vec{\tau}(\vec{\xi}\cdot\vec{\tau})$ if the deformation is plastic and $\vec{b}(\vec{\xi}) = \vec{\xi}$ if elastic. For this one-dimensional system, the eigenvalues $\lambda$ are 0 and $\pm c\sqrt{\vec{\xi}\cdot\vec{b}}$ with corresponding eigenvectors

$$\begin{pmatrix} 0 \\ \vec{\xi}^{\perp} \end{pmatrix} \quad \text{and} \quad \begin{pmatrix} -\lambda \\ \vec{b} \end{pmatrix} \tag{8}$$

These eigenvalues will be real provided that $h(|\vec{\tau}|) > |\vec{\tau}|^2\sin^2(\frac{\alpha}{2})$. Otherwise there is a direction that minimizes $\vec{\xi}\cdot\vec{b}$ and for which the eigenvalues are imaginary. This direction of extreme ill-posedness is the direction bisecting the angle made by $\vec{\tau}$ and $R\vec{\tau}$. That is, if $\vec{\tau} = |\vec{\tau}|(\cos\theta, \sin\theta)^T$, the extreme direction is $\vec{\xi} = (\cos\frac{\theta-\alpha}{2}, \sin\frac{\theta-\alpha}{2})^T$. For more details, see [7].

## 3. Shear Band

As explained above, shear bands originate at points of ill-posedness. The shear bands are idealized as stationary points of discontinuity in a weak solution of (4)(5). If $\vec{n}$ is the vector normal to the band, the normal component of the stress ($\sigma = \vec{\tau}\cdot\vec{n}$) is continuous across the band, while the tangential component ($\omega = \vec{\tau}\cdot\vec{n}^{\perp}$) may suffer a jump. The variables $\sigma_b$ and $\omega_b$ inside the band are related to the outside variables by a differential-jump relation:

$$\partial_t\vec{\tau}_b = A(\vec{\tau}_b)\begin{pmatrix} [v]/\delta \\ 0 \end{pmatrix} \tag{9}$$

where $\vec{\tau}_b = (\sigma_b, \omega_b)^T$, $[v]$ is the jump in the velocity across the band and $\delta$ is a "grain diameter" parameter. This equation provides the evolution of the stress inside the shear band.

## 4. Numerical Algorithms

Let $\gamma_c$ be the root to the equation $h(\gamma) = \gamma^2 \sin^2(\frac{\alpha}{2})$. For those points in the domain where $\gamma(t,x,y) < \gamma_c$, the system is hyperbolic and the eigenvalue-eigenvector study of section 2 is valid. The algorithm is organized in two blocks: the first one corresponds to the integration of the cells where the system is still hyperbolic ($\gamma < \gamma_c$). This is done via a second order algorithm based on Godunov methods. The second block consists of updating the cells intersected by the shear bands ($\gamma \geq \gamma_c$) and surrounding cells, which are expected to be affected by the presence of the shear band. This part of the algorithm is first-order accurate.

**4.1. Calculation before the formation of the shear band.** We momentarily assume that the states at the cell boundaries ($x = x_i = i\Delta x$ or $y = y_j = j\Delta y$) at the half timestep $t = t_n + \frac{1}{2}\Delta t$ are known. We refer to those states by $U^{n+\frac{1}{2}}_{i+\frac{1}{2},j}$ and $U^{n+\frac{1}{2}}_{i,j+\frac{1}{2}}$, where $U = (v, \tau_1, \tau_2, \gamma)^T$. The momentum equation (1) is in conservation form and we can write the usual Godunov type algorithm to update the velocity at a new time:

$$v^{n+1}_{i,j} = v^n_{i,j} + \frac{\Delta t}{\Delta x \Delta y}\left\{\Delta y\left[(\tau_1)^{n+\frac{1}{2}}_{i-\frac{1}{2},j} - (\tau_1)^{n+\frac{1}{2}}_{i+\frac{1}{2},j}\right] + \Delta x\left[(\tau_2)^{n+\frac{1}{2}}_{i,j-\frac{1}{2}} - (\tau_2)^{n+\frac{1}{2}}_{i,j+\frac{1}{2}}\right]\right\}. \tag{10}$$

Since the constitutive relations are in conservation form only while the material deforms elastically (but not for plastic deformations), the update of the stress variables cannot be done via a Godunov type algorithm. We integrate (5) along a particle path (similar to [9]), and since the motion is only on the $z$-direction (particles do not move in the $xy$-plane), this integration reduces to a simple integration in time for constant $x$ and $y$. To perform this integration first we approximate $\operatorname{grad} v$ in (5) by

$$\operatorname{grad} v \approx \frac{[\vec{\tau}]}{[x,y]}(\equiv)_d \begin{pmatrix} \dfrac{v^{n+\frac{1}{2}}_{i+\frac{1}{2},j} - v^{n+\frac{1}{2}}_{i-\frac{1}{2},j}}{\Delta x} \\ \dfrac{v^{n+\frac{1}{2}}_{i,j+\frac{1}{2}} - v^{n+\frac{1}{2}}_{i,j-\frac{1}{2}}}{\Delta y} \end{pmatrix} \tag{11}$$

and then we integrate numerically

$$\partial_t \vec{\tau} = A(\vec{\tau})\frac{[\vec{\tau}]}{[x,y]} \tag{12}$$

from $t = t_n$ to $t = t_n + \Delta t$. We notice that for elastic deformations, the integration of (12) is equivalent to an algorithm of Godunov type as that of (10).

The states $U^{n+\frac{1}{2}}_{i+\frac{1}{2},j}$ and $U^{n+\frac{1}{2}}_{i,j+\frac{1}{2}}$ are calculated via a one dimensional Riemann Solver [3, 4] and characteristic tracing algorithm [2, 8, 9] that incorporates transverse flow corrections as to achieve second order accuracy in space and time as well as stability.

**4.2. Integration algorithm near the shear band.** We define, geometrically, a shear band as an oriented curve in the $xy$-plane, whose intersection with a given cell is either empty or a segment of a straight line dividing the cell in two disjoint regions. That is we do not allow the shear band to end in the interior of a cell. These segments are called bonds and the intersection of the shear band with grid lines are called points.

The shear band is treated as an internal boundary where the stress evolves according to a particular evolution equation (9) as established in [7]. The approach used here follows traditional front tracking techniques [1] [5] with modifications proper to this problem: the tracked front is neither a hyperbolic wave nor does it divide the domain into unconnected domains. At the shear band the approximated solution is first order accurate. We organize the description of the method as follows: (a) averaging of states near the band, (b) update of states at the band, (c) recalculation of fluxes at and near the band and (d) integration on subcells and cells near the band.

For each cell intersected by a shear band, the eight surrounding cells will need to be updated again to account for the influence of the shear band. Let the $(i_b, j_b)$ cell be crossed by a shear band. We will refer to this cell as $C_b$ and the bond, portion of the shear band in the cell, as $I_b$. For later use we define the box centered at $C_b$, $B = [i_b - 1, i_b + 1] \times [j_b - 1, j_b + 1]$, and $B_b = B - (i_b, j_b)$. Associated with the bond $I_b$ we have information proper of the band:
- the states $U_b$ at the shear band.
- the states $U_b^L$ and $U_b^R$ at the sides of the band at time $t_n + \Delta t/2$,
- the states $U^L$ and $U^R$ on the subcells of cell $C_b$
and that of surrounding cells, $U_{i,j}$ for $(i,j) \in B$. The normal to the band, $\vec{n}$, is used to to determine if a cell, or portion of a cell, is to the left or right of the band. For the cells next to the tips of the bands, and only for the purpose of assigning left and right areas to these cells, we extrapolate the band at its endpoints by one or two cells in the direction of the last bond.

(a) Averaging of states. In what follows, we will refer to a left or right state with the index $S = L, R$. Since the side states $U^S$ correspond to subcells whose area can be very small, we average these states according to a weighted interpolation [1] :

$$\hat{U}^S = \frac{A^S_{i_b,j_b}}{\Delta x \Delta y} U^S + \left(1 - \frac{A^S_{i_b,j_b}}{\Delta x \Delta y}\right) \frac{\sum_{(i,j)\in B_b} A^S_{ij} U^S_{ij}}{\sum_{(i,j)\in B_b} A^S_{ij}},$$

where $A^S_{i,j}$ is the area of the portion of the cell $C_{i,j}$ to the $S$ side of the band.

(b) Updating of states at the band. We denote by $\sigma_b^n$, $\omega_b^n$, $\gamma_b^n$ the stress variables inside the band at $t = t_n$. We integrate (9) from $t_n$ to $t_n + \Delta t$, where $[v] = \tilde{v}_b^R - \tilde{v}_b^L$ and $\tilde{v}_b^S$ are the velocities of the states at the sides of the band at time $t_n$. These velocities are obtained as the result of tracing one parameter wave curves, with $\sigma$ as the parameter, from the side states $\hat{U}^S$ to $\sigma = \sigma_b^n$. The variables at the end of this integration are $\sigma_b^{n+1}$, $\omega_b^{n+1}$, $\gamma_b^{n+1}$. For the next step we need the value of $\sigma_b$ at a half-time step. We approximate this value by $\sigma_b^{n+1/2} = (\sigma_b^n + \sigma_b^{n+1})/2$ and identify $\sigma_b^R = \sigma_b^L = \sigma_b^{n+1/2}$.

(c) Calculation of fluxes. By tracing the one parameter wave curves, with $\sigma$ as the parameter, from the side states $\hat{U}^S$ to $\sigma = \sigma_b^S$ we obtain an approximation of the states $U_b^S$ at the sides of the band at $t = t_n + \Delta t/2$. We use these states to find the fluxes at the band. To calculate the fluxes at cell edges in $B$, to the left and right of the band, we repeat the calculation of $U^{n+\frac{1}{2}}_{i+\frac{1}{2},j}$ and $U^{n+\frac{1}{2}}_{i,j+\frac{1}{2}}$ as in section 4.1 (though this time with only first order accuracy) where we have replaced $U_{i_b,j_b}$ by $\hat{U}^S$ and $U_{ij}$ by $U^S_{ij}$ for $(i,j) \in B$.

(d) Integration near the band. If we denote by $d^S_{i+1/2,j}$ (resp. $d^S_{i,j+1/2}$) the length of the $(i+1/2, j)$ (resp. $(i, j+1/2)$) boundary on the $S$ side of the band and $d_b$ the length of the bond segment, the momentum equation is integrated on the $S$ subcell to

$$\begin{aligned} A^S_{i_b,j_b}\left[(v^S)^{n+1}_{i_b,j_b} - (v^S)^n_{i_b,j_b}\right] = \Delta t \Big[ & d^S_{i_b-\frac{1}{2},j_b}(\tau_1^S)^{n+\frac{1}{2}}_{i_b-\frac{1}{2},j_b} - d^S_{i_b+\frac{1}{2},j_b}(\tau_1^S)^{n+\frac{1}{2}}_{i_b+\frac{1}{2},j_b} + \\ & d^S_{i_b,j_b-\frac{1}{2}}(\tau_2^S)^{n+\frac{1}{2}}_{i_b,j_b-\frac{1}{2}} - d^S_{i_b,j_b+\frac{1}{2}}\tau_2^S)^{n+\frac{1}{2}}_{i_b,j_b+\frac{1}{2}} + (-1)^S d_b \sigma_b^S \Big], \end{aligned} \tag{13}$$

where $(-1)^L = -1$ and $(-1)^R = 1$).

If we write $M^S$ for the RHS of (13) and $M_{i,j}$ as the corresponding quantity in (10), we would like to write

$$(v^S)^{n+1}_{i_b,j_b} = (v^S)^n_{i_b,j_b} + \frac{M^S}{A^S_{i_b,j_b}}. \tag{14}$$

But, if $A^S_{i_b,j_b}$ is too small, (14) would violate the CFL stability condition. Instead, we write

$$(v^S)^{n+1}_{i_b,j_b} = (v^S)^n_{i_b,j_b} + \frac{M^S}{\Delta x \Delta y}. \tag{15}$$

This expression for $(v^S)^{n+1}_{i_b,j_b}$ satisfies the CFL condition, but when we compute the integral of the momentum equation in the region $C^S_b \times [t_n, t_n + \Delta t]$ and compare with (13) we observe that there is an excess of mass flux that is given by

$$M^S - A^S_{i_b,j_b}((v^S)^{n+1}_{i_b,j_b} - (v^S)^n_{i_b,j_b}) = M^S(1 - \frac{A^S_{i_b,j_b}}{\Delta x \Delta y}). \tag{16}$$

In order to be conservative in the region, we need to put the above excess "mass-flux" back into the algorithm. There are several techniques to carry out this mass redistribution. We partially follow the ideas of [1] with some variations in the sense that we perform a weighted area redistribution. The fact that the front is not hyperbolic, precludes a wave decomposition at the front, and the fact that the material presents a sharp discontinuity in the displacement indicates that transfer of "mass-flux" across the discontinuity is not proper. We now update the cells in $B$ by

$$v^{n+1}_{i,j} = v^n_{i,j} + \frac{M_{i,j}}{\Delta x \Delta y} + \sum_S \sum_F \left( M^S(1 - \frac{A^S_{i_b,j_b}}{\Delta x \Delta y}) \frac{1}{\sum_{B_b} A^S_{m,n}} \right) \tag{17}$$

if the shear band does not intersect $C_{i,j}$, and otherwise by

$$(v^S)^{n+1}_{i,j} = (v^S)^n_{i,j} + \frac{M^S_{i,j}}{\Delta x \Delta y} + \sum_F \left( M^S(1 - \frac{A^S_{i_b,j_b}}{\Delta x \Delta y}) \frac{1}{\sum_{B_b} A^S_{m,n}} \right) . \tag{18}$$

The sum $\sum_F$ is over all the band bonds that affect the $(i,j)$ cell. A similar process is done for the stress update.

**4.3. Initialization of the shear band cell.** When the total stress $\gamma$ reaches the critical value $\gamma_c$ at some cell $(i_b, j_b)$ and time $t_0$, a shear band is introduced in that cell. This can be due either to a shear band growing into a new cell or by the formation of a new shear band. Both cases are treated similarly. The direction of extreme ill-posedness for system (4)(5) is taken to be the normal direction to the shear band being initialized at that point. As seen above, this normal is $\vec{n} = (\cos\frac{\theta-\alpha}{2}, \sin\frac{\theta-\alpha}{2})^T$, where $\theta$ is the angle that the stress vector at that point makes with the positive $x$-axis. The exact placement of the band in the cell is done by: (a) continuation of a previous band, if present, from the boundary cell, or (b) locating a local maximum of $\gamma(t_0, x, y)$ in the cell $(i_b, j_b)$.

It may occur that during a single timestep, the states at several cells enter the region of ill-posedness. These cells may be associated with different shear bands or one single band growing rapidly since there is no a-priori limit in the rate of growth of the band. This potential difficulty is solved by integrating the stress at the "new" shear band cells at time subintervals. We explain the process: After a regular time step $[t_n, t_n + \Delta t]$, we sweep over all the cells which were not intersected by shear bands at $t = t_n$. We mark those cells, $C_1, \ldots, C_m$, where the stress has gone beyond the critical yield value $|\vec{\tau}| = \gamma_c$.

We write $\gamma(t,k)$ for the solution of (12) at each $C_k$ in $[t_n, t_n+\Delta t]$. For each $k$ we find the first $t_k$ such that $\gamma(t_k,k)=\gamma_c$ and label $t^*_{k_b}=\min_{k=1,\ldots m} t_k$. We redo the integration up to $t^*_{k_b}$ at the $C_k$ cells and the cells intersected by the shear band. This will give us the first cell $C_{k_b}$ in which to place a shear band as discussed above. We now repeat the above process from time $t=t^*_{k_b}$, adding, if necessary, new cells to the collection of marked cells until we exhaust the time interval. Although the process is potentially computationally intensive it is performed only during a small portion of the simulation.

With this process we take into account the effect of newly formed shear bands on their neighboring cells, either by accelerating the loading rate (and possibly introducing new band cells) or by unloading the nearby cells (and eliminating extraneous shear bands).

## 5. Examples

In this test run we consider a uniformly loaded sample with constant stress throughout the domain $\tau_1=.820352871$, $\tau_2=.409702741$ and $\gamma=.945303919$. The initial velocity is linear in the $x$-direction and constant on the $y$-direction, $v(0,x,y)=.05(x-.5)$, for $0<x,y<1$. If the material is homogeneous, the deformation, at all times, will consist of a velocity which is constant on time and stress that, although changing in time, remains constant in space (see [7]) . We introduce an inhomogeneity in the sample at the origin: $\alpha=.475$ everywhere except at the cell at the center of the domain and cells inmediatly above and below for which we set $\alpha=.5$. At short time after initialization, a shear band is formed in those cells. This band grows diagonally through the domain. We show two snapshots of the contours for the velocity (to the right) and $\gamma$ (to the left), when the shear band has grown half-way through the domain ( Figure 1) and after it has reached the boundaries of the domain (Figure 2).

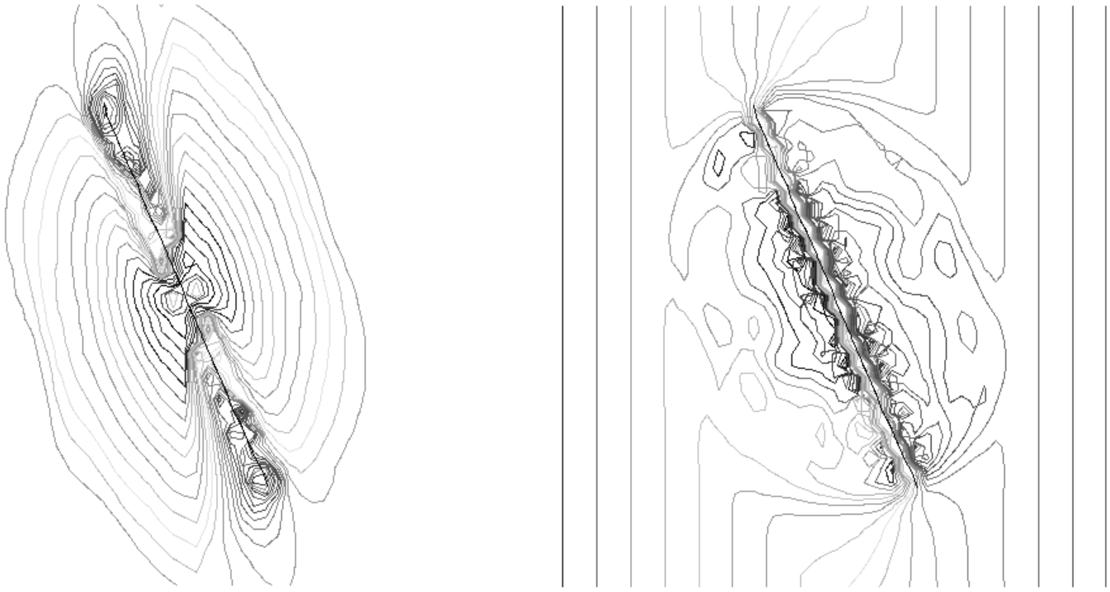

Figure 1. $\gamma$ and $v$ contour lines at intermediate time.

Some features to be noticed are: (a) the localization of high stress in the direction, and precceding, the shear band, (b) the unloading of the material in the direction orthogonal to the shear band and (c) the localization of the variation (jump) in the velocity at the shear band. All these phenomena agree with analytical and/or numerical studies performed for one-dimensional deformations ([4], [6], [7]).

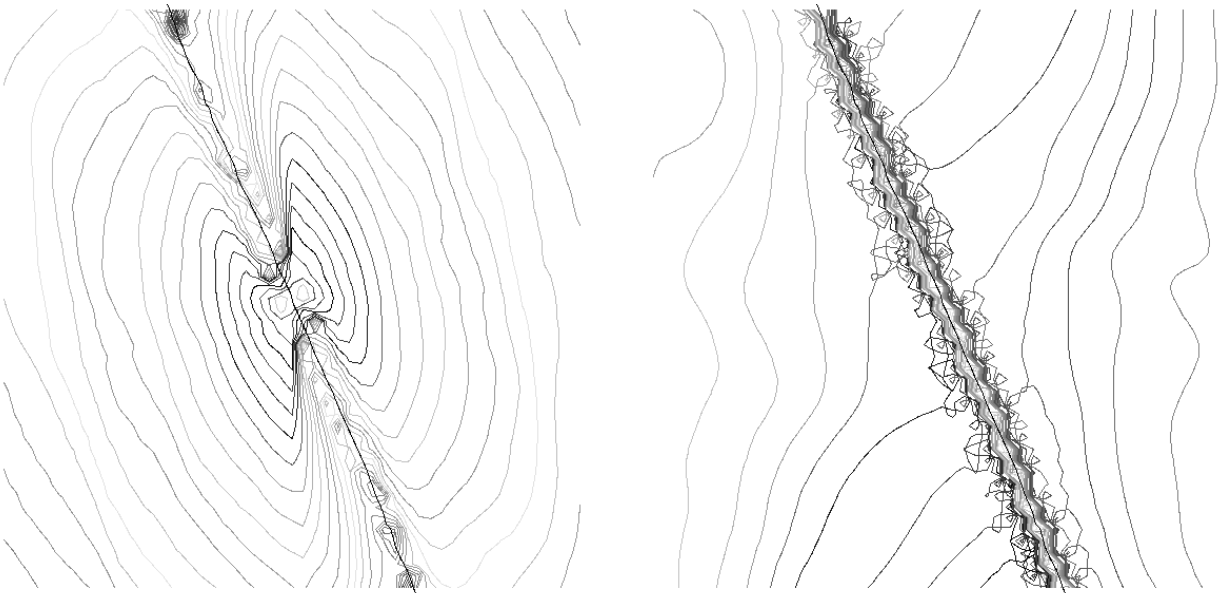

FIGURE 2. $\gamma$ and $v$ contour lines at larger time.

## REFERENCES


1. I-L. Chern and P. Colella, *A conservative front tracking method for hyperbolic conservation laws*, Tech. Report UCRL-97258, Lawrence Livermore National Laboratory, Lawrence Livermore National Laboratory, Berkeley, CA 94720, July 1987.
2. P. Colella, *Multidimensional upwind methods for hyperbolic conservation laws*, Journal of Computational Physics **87** (1990), 171–200.
3. X. Garaizar, *Numerical computations for antiplane shear in a granular flow model*, Quarterly of Applied Mathematics **52** (1994), 289–309.
4. X. Garaizar and D. Schaeffer, *Numerical computations for shear bands in an antiplane shear model*, J. Mech. Phys. Solids **42** (1994), no. 1, 21–50.
5. J. Glimm, E. Isaacson, D. Marchesin, and O. McBryan, *Front tracking for hyperbolic systems*, Advances in Applied Mathematics **2** (1985), 91–119.
6. D.G. Schaeffer M. Shearer, F.X. Garaizar and J. Trangenstein, *Numerical computations for shear bands in an antiplane shear model*, Annual ARO Conference on Applied Mathematics and Computing, vol. ARO 94-1, 1994, pp. 15–28.
7. D. G. Schaeffer, *A mathematical model for localization in granular flow*, Proceedings of the Royal Society of London **436** (1992), 217–250.
8. John A. Trangenstein, *A second-order godunov algorithm for two-dimensional solid mechanics*, Computational Mechanics **13** (1994), 343–359.
9. John A. Trangenstein and P. Colella, *A higher-order godunov method for modeling finite deformation in elastic-plastic solids*, Comm. Pure Appl. Math. **44** (1991), 41–100.



CENTER FOR RESEARCH IN SCIENTIFIC COMPUTATION AND DEPARTMENT OF MAT HEMATICS, BOX 8205, NORTH CAROLINA STATE UNIV., RALEIGH, NC 27695

*Current address*: Department of Mathematics, Box 90320, Duke University, Durham, NC 27706-0320

DEPARTMENT OF MATHEMATICS, BOX 90320, DUKE UNIVERSITY, DURHAM, NC 27706-0320